PHYSICAL REVIEW A **84**, 020502(R) (2011)

# $\nu_4$ band of $CH_4$ in helium nanodroplets: A probe of the dynamical response of a superfluid

Aakash Ravi,[*] Susumu Kuma,[†] Christopher Yearwood, Birinder Kahlon, Majd Mustafa, Watheq Al-Basheer, Katsunari Enomoto,[‡] and Takamasa Momose[§]

*Department of Chemistry, The University of British Columbia, Vancouver, British Columbia V6T 1Z1, Canada*

(Received 20 March 2011; published 26 August 2011)

The triply degenerate $\nu_4$ bending mode of methane in superfluid helium nanodroplets was observed at 7.7 $\mu$m by high-resolution infrared depletion spectroscopy. Five rotational transitions were detected, with a minimum linewidth of only 65 MHz. The observed lines showed slightly asymmetric line shapes, especially in the case of the $P(2)$ and $R(1)$ rotational lines. Analysis of the line shape indicates that the superfluid environment has a finite response time of a few nanoseconds to equilibrate upon rotational excitation of $CH_4$.

DOI: 10.1103/PhysRevA.84.020502 PACS number(s): 33.20.Ea, 67.25.dw, 33.70.Jg, 67.25.du

Over a decade of experiments has shown that molecules in superfluid helium nanodroplets rotate nearly freely, exhibiting quantized rotational states [1–3]. In fact, many insights into the nature of superfluidity can be directly obtained from the high-resolution rotational spectra of the guest molecules.

The embedded molecules typically show a reduction of the rotational constant, $B$, and an increase of the centrifugal distortion constant, $D$, in the droplet environment. These effects have been discussed in relation to collective excitations or destruction of the superfluid characteristics of the surrounding He, but the nature of the interactions causing these changes in molecular constants is still under considerable debate [2–7]. Heavy molecules, which exist in the so-called adiabatic following regime [3], have been studied extensively [8–10], but less work has been devoted to light molecules [11–14], in which destruction of the superfluid component around the molecules is expected to be suppressed, making them ideal probes of superfluid response.

Here, we have studied methane in helium droplets by high-resolution infrared (IR) depletion spectroscopy. Methane, which is a quintessential light molecule, is expected to be the best probe of superfluid phenomena, because the perturbation to the superfluid environment is minimal, owing to the weakly anisotropic interaction between $CH_4$ and He [7,15]. Moreover, the rotational energy of $CH_4$ (10.5 $cm^{-1}$ for $J = 1$ in the ground state) and the roton energy of bulk He (6 $cm^{-1}$) [3,16] are comparable, making direct coupling between the rotational excitation of $CH_4$ and the roton-maxon collective excitations of superfluid He feasible. We focused on the $\nu_4$ band of $CH_4$ since previous work which addressed the $\nu_3$ band [11–13] showed broad linewidths of 0.2 $cm^{-1}$, concealing detailed information about the structure and dynamics of the superfluid He. As the linewidths in the $\nu_4$ band of $CH_4$ are at least an order of magnitude smaller compared to those of the $\nu_3$ band in solid parahydrogen [17,18], this led us to expect a similar trend in He droplets.

Our experimental setup involves a continuous expansion of $^4$He gas though a small orifice (5 $\mu$m) maintained at a high stagnation pressure (2 MPa) and low temperature (11–16 K). The emerging molecular beam condenses into droplets, reaching a final temperature of 0.4 K via evaporative cooling [1]. The mean size of the droplet ($N_{He}$) is determined by the nozzle temperature $T_0$, with $T_0 = 11$ K corresponding to $N_{He} \sim 20\,000$, and $T_0 = 16$ K to $N_{He} \sim 2000$ [19]. The beam is skimmed and then enters a pickup cell, where each droplet is doped with a single $CH_4$ molecule (on average). Photons from a counterpropagating IR laser beam excite transitions of $CH_4$ in the droplets at resonant frequencies. Upon subsequent nonradiative relaxation of the excited molecule, roughly 200 atoms per excitation at $\lambda = 7.7$ $\mu$m evaporate, and this shrinkage of the droplet is detected as a depletion of a mass signal [1] in a quadrupole mass spectrometer.

A tunable external-cavity continuous-wave quantum cascade laser (Daylight Solutions, TLS-21077-MHF, with output power of 200 mW and frequency stability <30 MHz) was used as an IR source at 7.7 $\mu$m. Mode-hop-free fine tuning over 1 $cm^{-1}$ was performed using piezo actuation. The frequency of each scan was calibrated by the absorption of gaseous $CH_4$ [20] and the transmission signal of an air-spaced Ge Fabry-Pérot cavity (1-GHz free spectral range). The absolute frequency accuracy thus determined was better than 10 MHz. The length between the pickup cell and the ionization region was 1 m, which corresponds to an approximate 3-ms interaction time between the doped droplets and IR radiation as the longitudinal velocity of the droplets was ~300 m/s. To match this time scale, the IR radiation was chopped at 130 Hz with an optical chopper, and the depletion signal was demodulated by a lock-in amplifier.

Figure 1 shows an overall depletion spectrum of the $\nu_4$ band of $CH_4$ in He droplets at $T_0 = 16$ K. The spectrum shows five sharp lines, which are readily assigned to the $P(2)$, $P(1)$, $Q(1)$, $R(0)$, and $R(1)$ transitions. While the fundamental rotational energy of $CH_4$ is much higher than the temperature of the nanodroplets (0.4 K), the transitions from the $J = 1$ and $J = 2$ states are observed due to the nuclear spin modification of $CH_4$ [12].

From comparison to gas-phase data [20], there are some other lines which may be expected but are not observed experimentally in the droplet (see Fig. 2). The $P(2)$, $Q(2)$, and $R(2)$ lines in the $F_2$ nuclear spin symmetry are missing

[*]Present address: University of Waterloo, Waterloo, ON N2L 3G1, Canada.

[†]Present address: Research Core for Extreme Quantum World, Okayama University, Okayama 700-8530, Japan.

[‡]On leave from Department of Physics, University of Toyama, Toyama 930-8555, Japan.

[§]momose@chem.ubc.ca

 

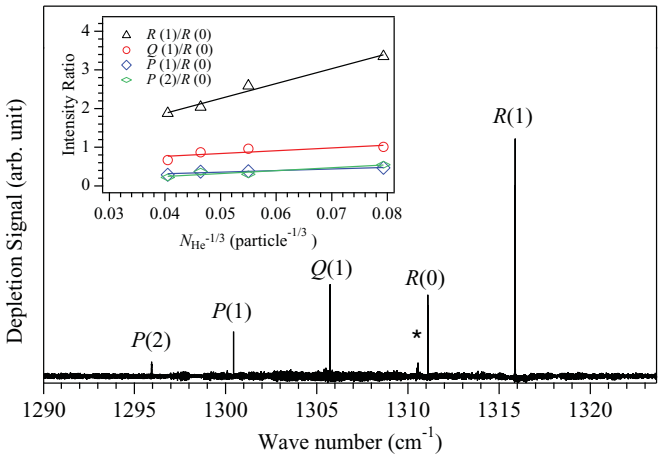


FIG. 1. (Color online) IR depletion spectrum of the $\nu_4$ band of $CH_4$ in He droplets at $T_0 = 16$ K. Rotational assignments are given for each peak. The peak marked by an asterisk (∗) is a transition of $(CH_4)_2$. (Inset) Ratios of the integrated line intensities relative to $R(0)$ as a function of $N_{He}^{-1/3}$.

due to fast rotational relaxation from the $J = 2$ state to the $J = 1$ state within the symmetry [21]. On the other hand, the $P(2)$ transition in the $E$ symmetry is observed as it occurs from the lowest rotational states in the $E$ symmetry [21]. In contrast, both $Q(2)$ and $R(2)$ in the $E$ symmetry are absent, although the $J = 2$ state is populated in the $E$ symmetry. The reason for the absence of the $R(2)$ $E$ transition may be due to the large rotational energy of the $J = 3$ upper state; this

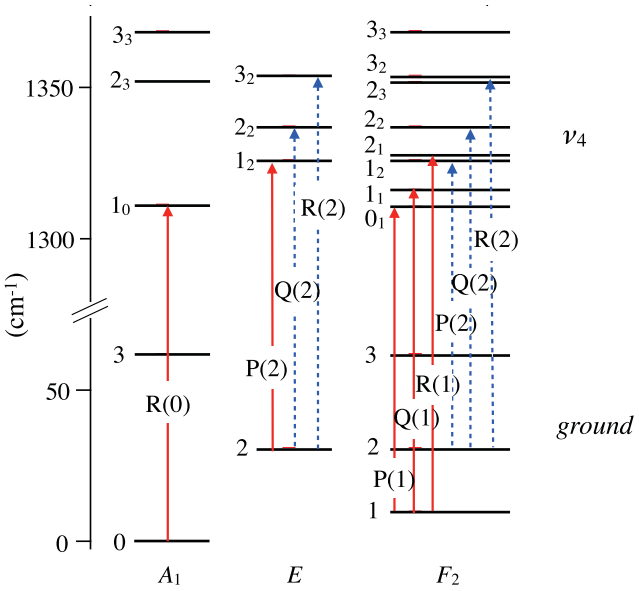


FIG. 2. (Color online) A schematic energy diagram of the rotation-vibration states of $CH_4$ for each nuclear spin state of $A_1$, $E$, and $F_2$. Each ground-state level is labeled with the corresponding rotational quantum number $J$. Similarly, each $\nu_4$ excited-state level is labeled with $J_R$, where $R$ is defined by the vector sum $\boldsymbol{R} = \boldsymbol{J} + \boldsymbol{\ell}$, with $\boldsymbol{\ell}$ being the vibrational angular momentum. The observed transitions are shown in red arrows and unobserved transitions are shown in blue dotted arrows.

facilitates efficient coupling to the elementary excitations of He, and thus fast relaxation occurs. The reason for the missing $Q(2)$ line is not known, but it is not seen in the $\nu_3$ band of $CH_4$ in He droplets either [12].

It is immediately visible from the spectrum in Fig. 1 that the peaks have anomalous intensities when compared to what would be expected theoretically. Nuclear spin statistics of $CH_4$ predicts an intensity ratio of the five lines as $P(2) : P(1) : Q(1) : R(0) : R(1) = 1 : 1 : 3 : 5 : 5$ [12], while the intensity ratio of laser-power-saturated lines is predicted to be $1 : 3 : 6 : 5 : 7.5$ [22]. The observed ratio of integrated intensities at $T_0 = 16$ K shown in Fig. 1 was roughly $2.8 : 2.4 : 5 : 5 : 17$; the $R(1)$ line is significantly more intense compared to the others.

Measuring the ratios at various $T_0$ values, i.e., various droplet sizes, revealed an approximately linear relationship with $N_{He}^{-1/3}$ (see inset of Fig. 1). The larger droplets give intensity ratios closer to the theoretical prediction by nuclear spin statistics. Our data clearly indicate that the nonradiative relaxation of the $v = 1$, $J = 2$ state is strongly affected by the size of the droplets, and the relaxation rate becomes faster in smaller droplets. The $N_{He}^{-1/3}$ dependence may imply that the anomalous intensities are due to surface effects [23], but they have yet to be fully understood.

The most striking difference between the present $\nu_4$ transitions and the $\nu_3$ transitions reported previously is the linewidth. Figure 3 shows expansions of each transition. The narrowest linewidth in $\nu_4$ is 65 MHz (full width at half maximum, FWHM) for the $Q(1)$ transition at $T_0$ = 11 K. The corresponding $Q(1)$ transition in $\nu_3$ has a linewidth of 11 GHz. All $\nu_4$ lines are more than two orders of magnitude narrower than the corresponding $\nu_3$ lines. The broad linewidths in the $\nu_3$ band are accounted for by fast vibration-vibration relaxation [24], as there are some vibrational states, such as the $\nu_2 + \nu_4$ and $2\nu_4$ states, whose energy is close to but slightly less than that of the $\nu_3$ state at 3020 cm$^{-1}$. Since the $\nu_4$ state

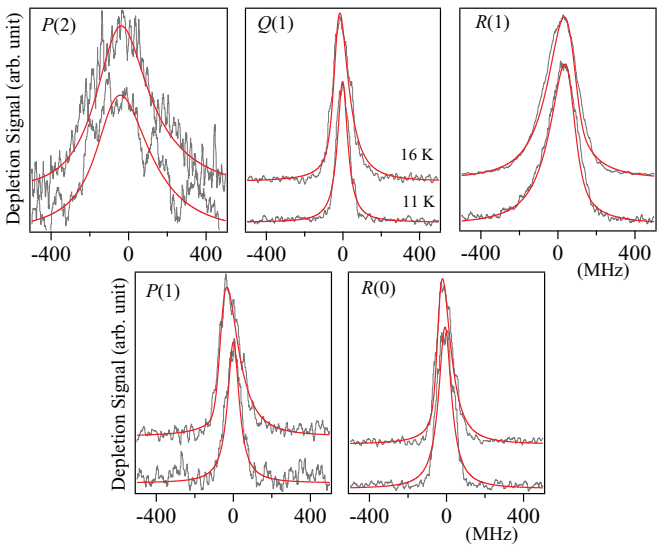


FIG. 3. (Color online) Line shapes of observed peaks; gray traces are the experimental spectra, and the red traces are fits to the model. In each panel, the upper and lower traces correspond to the spectra at $T_0 = 16$ and 11 K, respectively.

is the lowest excited vibrational state, no fast intramolecular vibrational relaxation occurs. It is also noted that the stretching $\nu_3$ mode perturbs surrounding He atoms more than the bending $\nu_4$ mode, which makes the relaxation faster in the $\nu_3$ mode than in $\nu_4$.

Upon closer examination of the observed lines, we noticed that some of the lines exhibited asymmetric line shapes. At $T_0 = 11$ K, the $P(2)$ line has a clear asymmetric tail toward higher frequencies, while the $R(1)$ has a low-frequency tail. The $P(1)$, $Q(1)$, and $R(0)$ lines are more or less symmetric at $T_0 = 11$ K. The $P(1)$ and $R(0)$ lines become slightly asymmetric, tailing toward higher frequencies in smaller droplets produced at $T_0 = 16$ K.

Similar line asymmetries have been reported for heavy molecules such as $SF_6$ [25] and OCS [9] in He droplets. In smaller droplets of $N_{He} = 200$ to 1000, all rotational lines showed a blue tailing for both molecules, which has been attributed to an inhomogeneous broadening due to the size distribution of the droplets, and the peak shifts are explained by the excluded volume theory [26]. In contrast, the "mirror image" line shapes of the $P$ and $R$ branches of OCS in large droplets toward the vibrational band origin have not been explained clearly until recently. van Staveren and Apkarian [27] have interpreted the mirror image asymmetry for OCS in He droplets as arising from the chirping of effective rotational frequencies due to the delayed response of the surrounding He shell upon rotational excitation. We found that the model explains the line asymmetries for $CH_4$, a light rotor case, as well.

The line shape $I(\nu)$ of the frequency-domain spectrum is related to the time correlation function $c(t)$ of a dipole operator $\hat{\mu}$ via the Fourier transformation, $I(\nu) \propto \mathrm{Re}[\int_0^\infty c(t)e^{-2\pi i\nu t}dt]$, where $c(t) = \langle\hat{\mu}(0)\hat{\mu}(t)\rangle = \exp(2\pi i\nu' t)\exp(-2\pi\gamma t)$ with $\nu'$ and $\gamma$ being the frequency of the dipole oscillation and its decay rate, respectively. The value $2\gamma$ is the FWHM of the frequency domain spectrum. In condensed phase spectroscopy, when there is a lag in the response of environment upon photoexcitation, the frequency $\nu'$ becomes time dependent. We assume [27] that the change of $\nu'$ in time is given by $\nu'(t) = \nu_c + \Delta[1 - \exp(-2\pi\beta t)]$, where the frequency $\nu'$ changes from $\nu'(0) = \nu_c$ to $\nu'(\infty) = \nu_c + \Delta$. The parameter $\beta$ represents the damping of the frequency chirping.

The observed spectral lines in Fig. 1 at $T_0 = 11$ K were analyzed by this model with $\nu_c$, $\Delta$, $\beta$, and $\gamma$ as parameters for a least-squares fitting. The determined parameters are listed in Table I. As shown in Fig. 1 with red traces, the model reproduces the observed shape quite well. The parameter $\Delta$ for $P(1)$, $Q(1)$, and $R(0)$ was fixed to zero, as the line shapes are almost symmetric.

At $T_0 = 11$ K, the parameter $\Delta$ is about 60 MHz for both $P(2)$ and $R(1)$ lines, but with opposite sign. The up-chirp ($\Delta > 0$), which is associated with $R(1)$ ($\Delta J = 1$), and down-chirp ($\Delta < 0$), which is associated with $P(2)$ ($\Delta J = -1$), imply that $d\omega_{CH_4}/dt > 0$ after the excitation in the former case, and $d\omega_{CH_4}/dt < 0$ in the latter, where $\omega_{CH_4}$ is the angular velocity of the rotor. The temporal change of the frequency is associated with the change of the effective moment of inertia of the system, $I_{eff} = I_{CH_4} + I_{He}$. As $I_{CH_4}$ is regarded as a constant, changes in $I_{eff}$ are attributed to changes in $I_{He}$, which in turn is caused by changes of the He environment around the rotor.

TABLE I. The fitted line shape parameters.

| | Parameters | | | |
|---|---|---|---|---|
| | $\nu_c$ ($cm^{-1}$)[a] | $\gamma$ (MHz) | $\Delta$ (MHz) | $\beta$ (MHz) |
| $P(2)$ | 1295.9475(25) | 160.5 | -68.8 | 47.5 |
| $P(1)$ | 1300.4409(11) | 36.1 | 0 | – |
| $Q(1)$ | 1305.7325(32) | 32.0 | 0 | – |
| $R(0)$ | 1311.0918(5) | 40.0 | 0 | – |
| $R(1)$ | 1315.8753(19) | 76.3 | 59.0 | 35.9 |

[a]The average value of several measurements. The standard deviation ($1\sigma$) for the last digit is given in parentheses.

The normal fraction around $CH_4$ is expected to be <5% [6,7], so the change in $I_{He}$ is mostly accounted for by the response of the superfluid component upon rotational excitation. Our analysis shows that $I_{eff}$ decreases as the rotational angular momentum $J$ increases. This is consistent with the nature of the rotor-superfluid interaction as a faster rotor couples more weakly to the environment [28]. However, the physical meaning of the parameter $\Delta$ for OCS (a heavy rotor case) [27] is different from that for $CH_4$. The change of $I_{He}$ in the OCS system is mostly due to the structural change of normal He atoms in the first solvation shell, and therefore it does not reflect the superfluid nature of the droplet. Naturally, the $\Delta$ values for OCS are significantly larger than those for the present system [27].

This analysis does not contradict the fact that the centrifugal distortion $D$ is a large positive value (see Table II). The sign and magnitude of $D$ are not simply related to the change of the moment of inertia because it is an effective constant which renormalizes the anisotropic potential effects into the kinetic parameters [4].

The damping rate $2\pi\beta$ of the chirping was ~250 MHz for both $P(2)$ and $R(1)$ at $T_0 = 11$ K, corresponding to a response time of 4 ns. The main contributions to this response time are thought to be from the exchange between normal and superfluid fractions and the rearrangement of superfluid He structures upon excitation. The slow response time (on the order of nanoseconds) is a hallmark characteristic of a superfluid system, as the motion of atoms in classical fluids happens on the time scale of picoseconds or faster [29]. Note that the OCS response time was found to be more than two orders of magnitude faster than [27] that of $CH_4$, as anticipated from the fact that the first He shell does not possess superfluid nature. Hence, this direct observation of the dynamical response time of a superfluid demonstrates that the high-resolution spectroscopy of a light rotor is a powerful tool for the study of microscopic superfluidity.

The shape in small droplets at $T_0 = 16$ K should be interpreted as a convolution of the effects from the chirped rotor as well as the statistical size distribution of the droplets. Although the mirror image was observed already at $N_{He} \sim 3000$ for OCS [9], it appears clearly only at $N_{He} > 20\,000$ for the $\nu_4$ transitions of $CH_4$. This supports our argument that the change in $I_{He}$ is mostly attributed to the response of superfluid component in the case of $CH_4$; for OCS, however, this change reflects the response of a classical He cluster. Since the superfluid state is characterized by long-range exchange of

TABLE II. Molecular parameters of $CH_4$ in He droplets and in the gas phase (in units of $cm^{-1}$).

| | $\nu_4$ | | $\nu_3$ |
|---|---|---|---|
| | He [present work] | Gas [30] | He [12] |
| $\nu_0$ | 1310.493(31) | 1310.761 | 3020.32(2) |
| $B''$ | 5.088(32) | 5.241 | 5.012(10) |
| $B'$ | 5.138(11) | 5.240 | 4.932(10) |
| $D$ | $2.86(89)\times10^{-2}$ | $1\times10^{-4}$ | $3.3(2)\times10^{-3}$ |
| $\zeta$ | 0.46575[a] | 0.46575 | 0.05583[a] |

[a]Fixed to the gas-phase value.

He atoms, the first He shell around $CH_4$ is more sensitive to the surface effect than the first He shell around OCS.

Table II shows the molecular parameters obtained by a least-squares fitting of the observed transition frequencies. We have used the same parameters and equations as described in Ref. [11]. We have fixed the Coriolis constant to the gas-phase value as in previous studies [12,17]. From Table II and Refs. [11,12], we see that the rotational constants are decreased by less than 5% from the gas-phase values in both states. The shift of the band origin in $\nu_4$ ($-0.27\ cm^{-1}$) is smaller than that of $\nu_3$ ($+0.83\ cm^{-1}$), indicating a weaker interaction strength between the vibrational motion of $CH_4$ and the surrounding He. The "effective" centrifugal distortion $D$ for $\nu_4$ in droplets is about ten times that for $\nu_3$.

In summary, we have observed extremely sharp lines in the $\nu_4$ band of $CH_4$ in He nanodroplets, and the observed line shapes show that the superfluid environment has a response time of a few nanoseconds to accommodate the change of rotational states of a central $CH_4$. As the He around $CH_4$ remains nearly completely superfluid, the $\nu_4$ band is an ideal probe of the dynamical response of a superfluid.

We are grateful to Prof. A. F. Vilesov and Dr. M. N. Slipchenko for helping us construct our droplet machine, and we wish to acknowledge Daylight Solutions for developing our laser system. This work is supported by an NSERC Discovery Grant and funds from CFI to CRUCS at UBC.

[1] J. P. Toennies and A. F. Vilesov, Angew. Chem. Int. Ed. Engl. **43**, 2622 (2004).
[2] F. Stienkemeier and K. K. Lehmann, J. Phys. B **39**, R127 (2006).
[3] M. Y. Choi, G. E. Douberly, T. M. Falconer, W. K. Lewis, C. M. Lindsay, J. M. Merritt, P. L. Stiles, and R. E. Miller, Int. Rev. Phys. Chem. **25**, 15 (2006).
[4] K. K. Lehmann, J. Chem. Phys. **114**, 4643 (2001).
[5] K. K. Lehmann and C. Callegari, J. Chem. Phys. **117**, 1595 (2002).
[6] N. D. Markovskiy and C. H. Mak, J. Phys. Chem. A **113**, 9165 (2009).
[7] R. E. Zillich and K. B. Whaley, J. Chem. Phys. **132**, 174501 (2010).
[8] M. Hartmann, R. E. Miller, J. P. Toennies, and A. Vilesov, Phys. Rev. Lett. **75**, 1566 (1995).
[9] S. Grebenev, M. Hartmann, M. Havenith, B. Sartakov, J. P. Toennies, and A. F. Vilesov, J. Chem. Phys. **112**, 4485 (2000).
[10] K. Nauta and R. E. Miller, J. Chem. Phys. **115**, 10254 (2001).
[11] K. Nauta and R. E. Miller, Chem. Phys. Lett. **350**, 225 (2001).
[12] H. Hoshina, D. Skvortsov, B. G. Sartakov, and A. F. Vilesov, J. Chem. Phys. **132**, 074302 (2010).
[13] S. Rudolph, G. Wollny, K. von Haeften, and M. Havenith, J. Chem. Phys. **126**, 124318 (2007).
[14] M. N. Slipchenko and A. F. Vilesov, Chem. Phys. Lett. **412**, 176 (2005).
[15] T. Momose, J. Chem. Phys. **107**, 7695 (1997).
[16] R. A. Cowley and A. D. B. Woods, Can. J. Phys. **49**, 177 (1971).
[17] T. Momose, M. Miki, T. Wakabayashi, T. Shida, M.-C. Chan, S. S. Lee, and T. Oka, J. Chem. Phys. **107**, 7707 (1997).
[18] H. Katsuki and T. Momose, Phys. Rev. Lett. **84**, 3286 (2000).
[19] J. Harms, J. P. Toennies, and F. Dalfovo, Phys. Rev. B **58**, 3341 (1998).
[20] S. Albert, S. Bauerecker, V. Boudon, L. R. Brown, J.-P. Champion, M. Loëte, A. Nikitin, and M. Quack, Chem. Phys. **356**, 131 (2009).
[21] B. H. Yang and P. C. Stancil, Eur. Phys. J. D **49**, 317 (2008).
[22] D. Skvortsov, D. Marinov, B. G. Sartakov, and A. F. Vilesov, J. Chem. Phys. **131**, 241103 (2009).
[23] K. von Haeften, T. Laarmann, H. Wabnitz, T. Möller, and K. Fink, J. Phys. Chem. A **115**, 7316 (2011).
[24] P. Hess, A. H. Kung, and C. B. Moore, J. Chem. Phys. **72**, 5525 (1980).
[25] M. Hartmann, N. Pörtner, B. Sartakov, J. P. Toennies, and A. Vilesov, J. Chem. Phys. **110**, 5109 (1999).
[26] J. Jortner and N. Ben-Horin, J. Chem. Phys. **98**, 9346 (1993).
[27] M. N. van Staveren and V. A. Apkarian, J. Chem. Phys. **133**, 054506 (2010).
[28] J. Manz, J. Am. Chem. Soc. **102**, 1801 (1980).
[29] I. V. Hertel and W. Radloff, Rep. Prog. Phys. **69**, 1897 (2006).
[30] A. G. Robiette, J. Mol. Spectrosc. **86**, 143 (1981).